ANNALS OF GEOPHYSICS, 68, 1, V113, 2025; doi:10.4401/ag-9175
OPEN ACCESS

Towards a probabilistic risk analysis due to volcanic-hazards at Mount Etna

Vera Pessina[*,1], Fabrizio Meroni[1], Elisa Varini[2], Marina Longoni[1], Laura Sandri[3], Alexander Garcia[3], Annalisa Cappello[4]

(1) Istituto Nazionale di Geofisica e Vulcanologia, Sezione di Milano, Milano, Italy
(2) Consiglio Nazionale delle Ricerche, IMATI, Milano, Italy
(3) Istituto Nazionale di Geofisica e Vulcanologia, Sezione di Bologna, Bologna, Italy
(4) Istituto Nazionale di Geofisica e Vulcanologia, Osservatorio Etneo, Catania, Italy

Article history: received October 2, 2024; accepted February 28, 2025

Abstract

Mount Etna is the largest active volcano in Europe and is renowned for its effusive and explosive eruptions, frequently accompanied by intense seismic activity. The densely urbanized area of Eastern Sicily (Italy), situated on the flanks of Mt. Etna, has been the focus of an innovative and comprehensive research project aimed at evaluating the potential volcano hazards and subsequent risks. Hazard scenarios were generated within the research project PANACEA (Probabilistic AssessmeNt of volCano-related multi-hazard and multi-risk at Mount EtnA) and they have been effectively employed in risk assessment for built-up areas and lifelines. The risk analyses were conducted for lava flow, tephra fall and volcanic earthquake hazards. Risk scenarios were assessed at different spatial scales, from the local one (at the resolution of the census track) to the sub-regional scale, defined as the union of some municipalities. Probabilistic damage scenarios were calculated with the aim of conducting a multi-hazard risk analysis, estimating direct losses in terms of structural damage, casualties and loss of functionality. A few examples of risk assessment are presented here to test the last step of the whole process developed in PANACEA.

Keywords: Multi-hazard; Risk; Probabilistic approach; Damage; Mt. Etna

1. Introduction

Assessing the potential effects of a volcanic eruption is a multifaceted process, since volcanoes are complex systems capable of generating numerous hazardous natural phenomena (Martí Molist, 2017; Loughlin et al., 2015). These include lava flows, tephra fallout, lahars, pyroclastic density currents and debris avalanches, which may sometimes interact and generate cascading effects over different temporal and spatial scales. The assessment of volcanic risks in densely populated areas has always been a very intricate issue (Zuccaro, 2008) due to the distinct characteristics of the phenomena associated with an eruption, which often manifest themselves through irregular temporal evolutions.

Numerous studies have been conducted to assess volcanic risk, the majority of which concentrated on a specific volcanic hazard (Spence et al., 2005; Jenkins et al., 2015; Bonadonna et al., 2021). The few available studies on multi-hazard risk assessment have given particular attention to the quantitative assessment of physical damage (Alberico et al., 2011; Alcorn et al., 2013; Pareschi et al., 2000; Zuccaro and De Gregorio, 2013; Alcozer-Vargas et al., 2022; Martín-Raya et al., 2024; Weir et al., 2024). In any case, whether studies on a single hazard or many hazards, it is widely recognized that comprehensive and multidisciplinary methods for assessing vulnerability associated with volcanic hazards remain a difficult issue (Bonadonna et al., 2018).

Mount Etna, situated at an elevation of over 3,400 m above sea level, dominates the eastern coast of Sicily and overlooks the metropolitan area of Catania, which has a population of over 777,700 inhabitants. In this area, most risk studies have been carried out considering only the seismicity. The seismic risk has been already addressed both for urban centers located on the slopes of the volcano (D'Amico et al., 2016; Sigbjörnsson et al., 2016; Pessina et al., 2021) and for the large city of Catania (Faccioli et al., 1999; Faccioli and Pessina, 2000; Spence and Le Brun, 2006), with reference to a complex and organized system of buildings (building heritage, schools, strategic structures) and lifelines (Meroni et al., 2016). Other more recent studies have focused on the assessment and mitigation of the risk from lava flows (Del Negro et al., 2019; Centorrino et al., 2021) and of fallout of ballistic blocks and bombs ejected from eruptive vents (Osman et al., 2019). However, a complete risk assessment of Etna must also take into account the frequent summit activity with vigorous ash emissions (Scollo et al., 2009; 2013) that can damage anthropic structures and cover cultivated and inhabited areas.

A multidisciplinary approach is therefore essential to assess the volcanic risk on Mount Etna, as its slopes can be affected by frequent tephra emissions, which have a negative impact on infrastructure, but also by lava flows and recurring earthquakes that have the potential to destroy man-made structures. These different types of hazard can occur simultaneously, as happened, for example, during the 2001 and 2002 eruptions (Neri et al., 2005).

In this paper, we present the first multi-hazard risk probabilistic analyses at Etna considering the effects of purely volcanic earthquakes, tephra fallout, and lava flows on the built environment (buildings, people and power lines), showing how studies of this type are fundamental for territorial planning in the context of natural risk prevention, but also for the management of the frequent seismic and volcanic emergencies. The damage caused by pyroclastic flows has not been considered since these events affect the summit area of the volcano with limited exposed elements (Zuccarello et al., 2025).

Our risk analyses are based exclusively on the hazards considered in the framework of the research project PANACEA (Probabilistic AssessmeNt of volCano-related multi-hazard and multi-risk at Mount EtnA). Specific examples of risk estimates are presented, whose values are indicative, but useful for a relative comparison of the risk levels produced by the different hazards. The use of different hazard scenarios, appropriately homogenized, in view of their practical application on the same exposed elements, is the real focus of this work, as the final step of a complete pathway from modelling, to hazard, up to risk.

This section continues by introducing the study area along with its associated exposure data, and the hazard scenarios developed within the PANACEA project. Section 2 describes the damage estimation models for buildings and lifelines; Section 3 reports some examples of probabilistic damage scenarios; Section 4 summarizes the major achievements, highlighting the overall purpose and suggesting possible directions for future research.

1.1 Study area and data collection

The study area is located in the south-east flank of Mount Etna, which is highly urbanized. In particular, we considered the six municipalities of Milo, Giarre, Riposto, Santa Venerina, Zafferana Etnea, and Acireale, covering an area of about 200 km^2 (Fig. 1a). These municipalities are the most likely to suffer severe impacts from volcanic eruptions and seismic crises, even simultaneously. The population of approximately 109,827 inhabitants (data as of 2024) is unevenly distributed in the municipalities: Acireale, Riposto and Giarre have a population density of ~1000-1200 inhabitants/km^2, while much lower densities are recorded in Zafferana Etnea (~120 inhabitants/km^2) and Milo (~61 inhabitants/km^2) (Fig. 1b).

The first step of the risk analysis included the identification of the elements exposed to volcanic products. In this framework, we have collected a large amount of data from regional and provincial government offices (Table 1), and organized it in a GIS, allowing complex analyses of vulnerability, damage and risk interaction to be carried out.

Themes	Data
Demographics	population
Building stock	residential, commercial, industrial
Essential facilities	hospital, schools, police and fire stations, hotels, municipal offices
Transportation	highways and bridges, state/provincial/city roads, railways and stations
Lifeline utility	potable water, wastewater, oil, gas, power, communication
Hazardous material	facilities housing industrial and hazardous material

Table 1. Inventory of elements at risk.

Among the collected data, we focused on residential buildings and the power distribution system, and on the assessment of their vulnerability to the various hazards (Meroni et al., 2022, Pessina et al., 2022).

A valuable source of information on building stock and demographic information is represented by the census data collected by the Italian Institute of Statistics (ISTAT), periodically updated and spatially detailed. For our analyses, we used the 2011 ISTAT data, since they are the only ones disaggregated by census section and therefore suitable for detailed vulnerability analyses. This assumption did not affect the final damage estimates. In fact, the comparison of the demographic variation between the 2011 ISTAT data and the updated data (ISTAT, 2024) showed limited fluctuations, ranging from –4.9% (in Giarre) to +2% (in Santa Venerina and Zafferana Etnea).

The residential buildings of the six municipalities under study are almost 26,200 and are subdivided in two categories based on the construction material: masonry and reinforced concrete (RC). Figure 1c illustrates the distribution of the prevalent typological structure of residential buildings and the location of the main roads. With the exception of

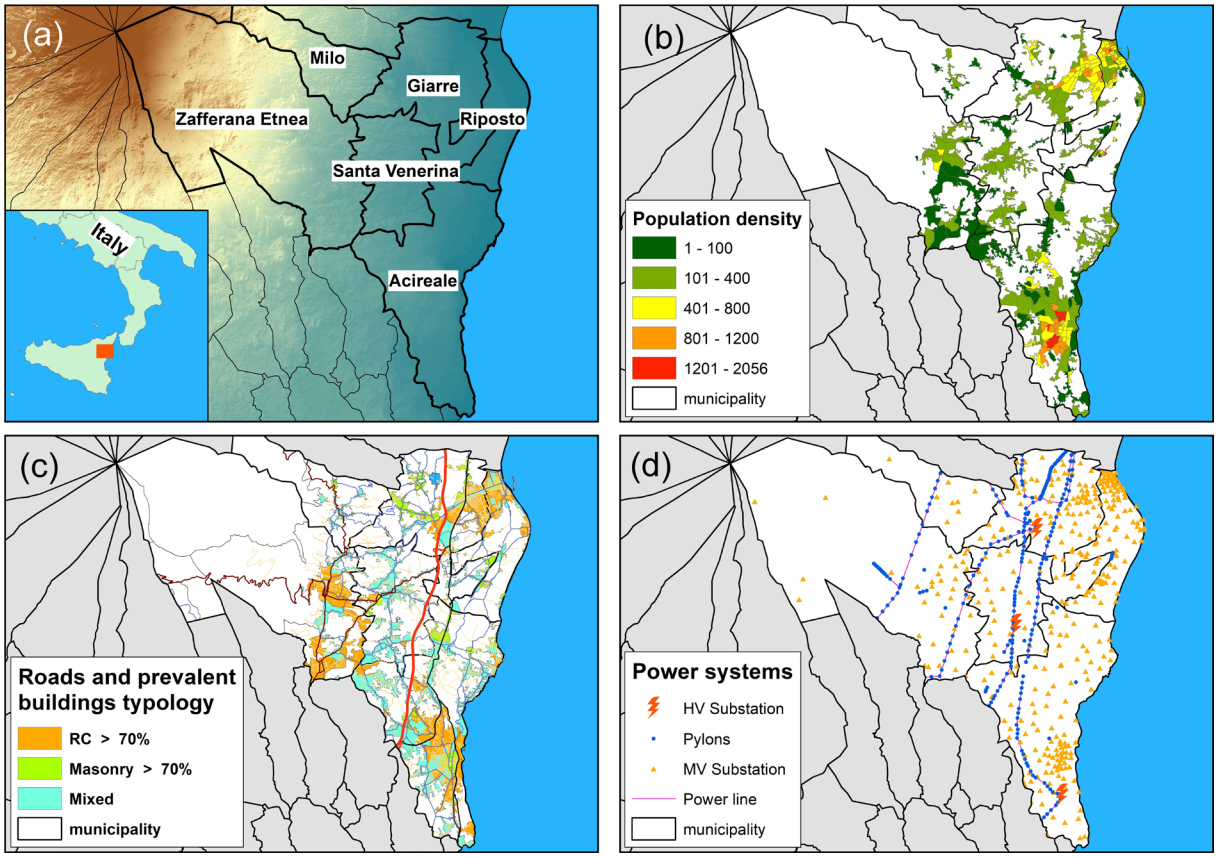

Figure 1. Examples of the inventory assets organized in a dedicated GIS. (a) The south-east flank of Etna, including the six municipalities of the study area. (b) The population density (inhabitant/km^2) per municipality, at the resolution of census track. (c) Typological characterization of residential buildings, at the resolution of the urbanized census track. (d) The electric power distribution system.

Zafferana Etnea and Milo, all municipalities exhibit a similar prevalence of masonry and reinforced concrete buildings. It is worth noting that the prevalence of reinforced concrete buildings in Zafferana Etnea is likely a consequence of the 1984 earthquake, which led to the demolition and subsequent reconstruction of numerous edifices in the area.

Data on the electric power system has been collected during the DG ECHO UPStrat-MAFA project (Sigbjörnsson et al., 2016). An electric power system is divided in a transmission system, that covers long distances at high voltages, and a more local distribution system, which directly connects homes via cables with voltages of 220-240 V for Europe. The system includes pylons and medium and high-voltage transformer substations (HV and MW substations) as main structures (Fig. 1d), which are considered for our risk analysis.

Network analysis capable of assessing the interaction of the power distribution systems with buildings or strategic structures is deferred to a subsequent in-depth phase.

1.2 Hazard scenarios overview

For our risk analyses, we considered three hazards associated to the eruptive activity of Etna: volcano-tectonic earthquakes, tephra deposits and lava flows, which have been studied in the framework of the PANACEA project. In the following paragraphs, we provide a brief description of the approaches used to assess each single hazard. Further details can be found in D'Amico et al. (2025), Scollo et al. (2025) and Cappello et al. (2025).

Seismic hazard

Seismic hazard was assessed based solely to local earthquakes, neglecting other related phenomena, such as the impact of surface faulting caused by outcropping fault planes (Neri et al., 2009) or the regional seismic tectonic events. The seismic analyses were carried out using the SASHA (Site Approach to Seismic Hazard Assessment) code (D'Amico and Albarello, 2008). For each studied site or point on a grid, the macroseismic history was calculated using the observed macroseismic data from the Catalogo Macrosismico dei Terremoti Etnei (CMTE, Azzaro and D'Amico, 2014), integrated with "virtual" intensity values estimated according to attenuation laws specifically developed for volcanic areas (Rotondi et al., 2016). The resulting probabilistic seismic hazard was expressed in terms of intensity, i.e., the probability $Prob(I)$ of an intensity I at each site was obtained for all $I = 1, \ldots, I_{MAX}$, where $I_{MAX} = 12$ is the maximum degree of the macroseismic scale.

To assess the damage to structures, the seismic hazard was then converted from intensity to Peak Ground Acceleration (PGA) using a new relationship specifically developed for the Etnean area (D'Amico et al., 2025):

$$\log_{10}(PGA) = 0.346 I_{EMS-98} - 0.190 \quad (1)$$

The error, $\sigma = \sigma_I$, associated with this new relationship depends on I, and its square was estimated for intensities III to IX as follows: $\sigma_3^2 = 0{,}547$, $\sigma_4^2 = 0{,}322$, $\sigma_5^2 = 0{,}168$, $\sigma_6^2 = 0{,}209$, $\sigma_7^2 = 0{,}106$, $\sigma_8^2 = 0.073$, and $\sigma_9^2 = 0.019$.

Tephra fallout hazard

For the tephra fallout, Scollo et al. (2025) analyzed separately the hazard from the tephra accumulated at the ground during flank eruptions and from the summit activity, and generated three maps: one for flank eruptions, one for summit eruptions, and one that considers both (hereinafter called "aggregated"). Hazard was assessed by using the TEPHRA2 model for the simulation of eruptive scenarios and considering the probability of future vent opening estimated by Sandri et al. (2024). Simulations were performed from several thousands of potential vents located on the Etna edifice, incorporating various wind fields to account for uncertainties in both vent position and meteorological conditions. The results of these simulations were processed to obtain hazard curves that represent the probability of tephra accumulation exceeding specified load thresholds (ranging from 0.1 to 1000 kg/m^2). These loads were converted into thicknesses using an average tephra density of 1000 kg/m^3.

Lava flow hazard

Lava flow hazard was assessed using a new probabilistic methodology based on a 4,000 years-long dataset of eruptions and accurate statistical analyses (Cappello et al., 2025). The methodology combines the probability of future vent opening (Sandri et al., 2024), the probabilities of occurrence of individual classes of eruptions, and the weighted combination of lava flow simulations. These simulations, based on representative scenarios for each eruption class, were performed using the physics-based GPUFLOW model (Cappello et al., 2022) on a satellite-derived Digital Surface Model (Ganci et al., 2023a). As well as tephra fallout, the results are two maps, one for flank and one for summit eruptions, which provide the likelihood that a specific area will be affected by lava flow inundation during specific time intervals. Moreover, an aggregated hazard map was also developed considering both kinds of eruptions.

2. Damage estimation models for buildings and lifelines

Regarding the damage assessment, hazard intensity is described quantitatively for seismic ground shaking and tephra deposits, while it is modelled as a binary phenomenon (affected or unaffected areas) for lava flows. In this latter case, we know that the resulting binary damage assessment could be overly simplistic (Meredith et al., 2022). However, it is a fairly strong assumption that the loss suffered by an infrastructure or building inundated by a lava flow is total, so the vulnerability can be set to one (Del Negro et al., 2019).

To calibrate damage models specific to the Etnean area and establish a comprehensive risk assessment procedure, we first generated deterministic damage scenarios (Pessina et al., 2024; Meroni et al., 2022).

2.1 Seismic actions on residential buildings

The damage assessment of residential buildings was addressed thanks to the availability of the 2011 ISTAT data and using the recent implemented damage assessment models (Dolce et al., 2021) adopted in the National Risk Assessment for Italy by the Department of Civil Protection. The damage assessment for other types of buildings (such as hospitals, schools, police and fire stations, hotels, municipal offices, etc.) was excluded at this stage, as the structures would require individual analysis using detailed structural models based on a significant amount of data currently unavailable.

The seismic vulnerability classes and damage levels for residential buildings were defined in accordance with the EMS-98 scale definition (Grünthal, 1998).

Different models were used to evaluate the seismic vulnerability classes and damage levels for both masonry and reinforced concrete buildings. According to these models, vulnerability was determined by a combination of structural typology, building age, and number of floors. Masonry buildings were assigned a vulnerability index ranging from A to D (Lagomarsino et al. 2021), while reinforced concrete buildings were classified as either C and D. The latter were further subdivided into three classes of buildings based on height (Rosti et al., 2021), resulting in a total of 10 vulnerability classes: four for masonry and six for reinforced concrete buildings (Table 2).

The fragility curves for masonry and reinforced concrete buildings, as defined by Lagomarsino et al. (2021) and Rosti et al. (2021), provided the probability of reaching damage levels *DL* for a given *PGA* value: $Prob(DL \mid PGA)$, where the damage levels range from *D1* (light damage) to *D5* (collapse), according to the EMS-98 scale definition.

Probabilistic seismic damage assessment was evaluated on the entire fragility curve for each vulnerability class shown in Table 2. The seismic risk *R* for *n* residential buildings classified in a given vulnerability class was assessed as:

$$R = n \cdot \int_0^{+\infty} Prob(DL|PGA) \cdot \left[\sum_{I=1}^{I_{MAX}} Prob(I) \cdot \phi\left(\frac{\log_{10}(PGA) - (0.346 \cdot I - 0.190)}{\sigma_I} \right) \right] dPGA, \quad (2)$$

where ϕ denotes the probability density function of the standard Normal distribution, and the mathematical summation enclosed in square brackets represents the conversion of the seismic hazard map from intensity to PGA (Eq. 1). Note that seismic hazard assessment was calculated at the centroid of each census section. This level of

Construction material	Vulnerability class			
Masonry	A	B	C	D
Reinforced concrete			C2-Low rise C2-Medium rise C2-High rise	D-Low rise D-Medium rise D-High rise

Table 2. Building classification scheme in the EMS-98 definition vulnerability classes.

resolution, which in densely populated areas corresponds to neighborhood or district resolution, was the maximum level of detail at which ISTAT data on buildings and population were available. Consequently, damage was also calculated at census plot level to optimize the use of high-resolution building data.

2.2 Tephra fallout on residential buildings

To assess the vulnerability of building roofs to tephra fall load, we applied the model of Spence et al. (2005), classifying roofs into four classes based on their probable resistance to tephra fall loads: weak (WE), medium weak (MW), medium strong (MS), and strong (ST). These classes are defined on an equally spaced logarithmic scale of resistance, with average resistance of 2kPa for WE, 3kPa for MW, 4.5kPa for MS, and 7kPa for ST (Fig. 2a).

As the dataset from the ISTAT census lacked information on the type of roofs, we exploited data from the AeDes modules (Baggio et al., 2007) and the classification of coverages obtained by satellite images. The AeDes forms, collected by the Department of Civil Protection of Sicily (DPCR), provide data on buildings damaged during the 2002 seismic crisis in a number of municipalities, covering a wider geographical area than the one considered in this study (Torrisi, 2018). The roof cover classification for the Etna urban area through satellite images was developed by Ganci et al. (2023b). High-resolution Worldview multispectral images were analyzed with a two-stage machine learning approach: the first stage provided a supervised classification for land use, while the second stage identified terraces and pitched roofs.

A preliminary classification into four vulnerability classes was performed using the following Aedes data: building typology, construction period, predominant horizontal structural components and roof structure (weight and thrusting/non-thrusting on the supporting walls). For instance, the ST roof class was assigned to buildings with a "*Flat reinforced concrete roof designed for access; recent, good quality construction, younger than 20 years*" (see classes definition in Spence at al., 2005). The percentage distribution of the roofs' vulnerability classes obtained through AeDes data is shown in Fig. 2b.

By assuming consistency in building typologies and construction methods on the eastern slope of Etna, this distribution can also be regarded as fairly accurate at the census tract level. To enhance the results at this finer spatial scale, we resort to the high resolution of the satellite images providing the percentage distribution of terraces and pitched roofs for each census tract.

The Spence model, applied to the roof typologies of the Etnean area, enabled a clear association of the WE and MW classes to the pitched roofs, and the ST class with terraces. In contrast, roof types for MS class remain uncertain, as this class encompasses flat reinforced concrete roof, sloping reinforced concrete roof, and good quality sheet roof on timber rafters. For each census track, we decided to subdivide the AeDes percentage of MS roofs (14%) into two equal parts, between pitched roofs and terraces. In this way, all the buildings in the census track are classified into two main groups based on the roof type, pitched roof and terrace. Within each group, the roofs were proportionally redistributed between the vulnerability classes according to the roof percentage provided by the AeDes data (Fig. 2b).

The percentage distribution was estimated for each class of roof vulnerability within the study area. As an example, Fig. 2c shows the final percentage distribution of the medium weak class (MW) in the inhabited localities of the study area.

Finally, the fragility functions proposed by Spence et al. (2005), shown in Fig. 2a, were applied to simulate the damage scenario for a specific tephra fallout hazard map. This approach was employed to evaluate a set of probabilistic risk maps for tephra fallout in the built-up areas.

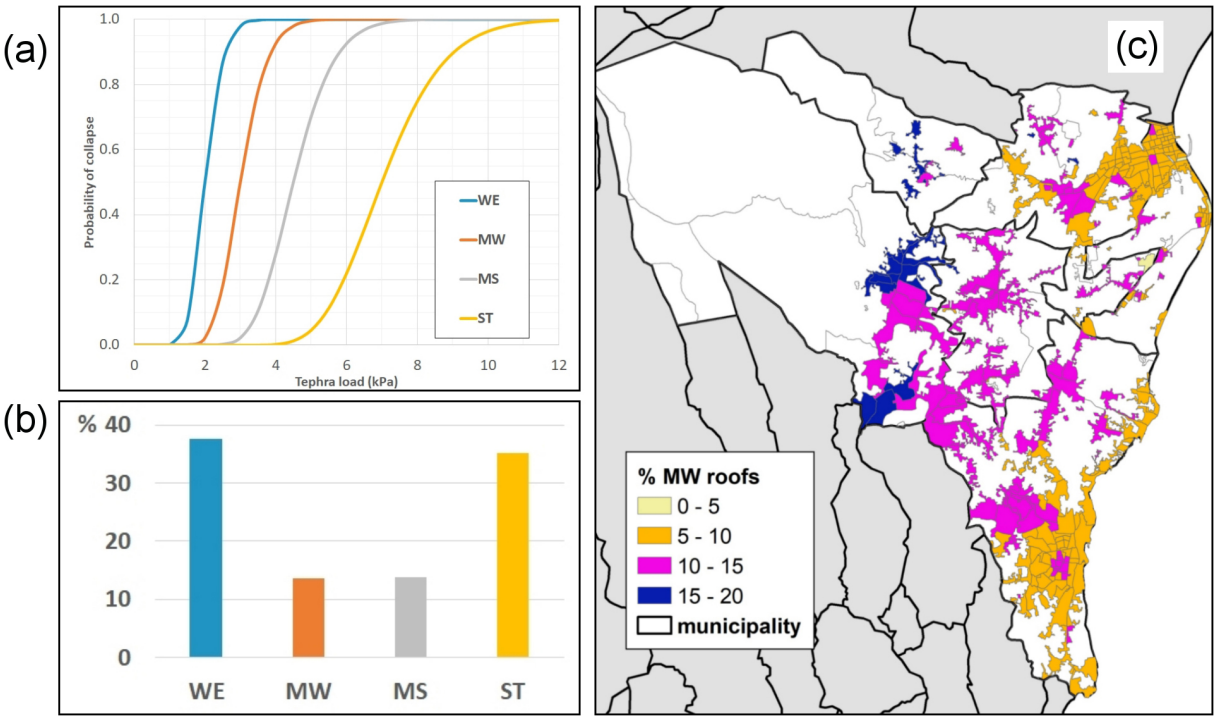

Figure 2. (a) Fragility curves for the roof vulnerability classes. (b) Percentage distribution of the roofs based on AeDes data according to the classification proposed by Spence et al. (2005) for weak (WE), medium weak (MW), medium strong (MS) and strong (ST) roofs. (c) Incidence of the presence of medium weak (MW) roofs in the inhabited areas of the 6 municipalities.

2.3 Tephra fallout on power distribution system

In the case of tephra loads, damage to the power distribution system depends on the thickness of the deposited material. Threshold values were used to define the damage states (Jenkins et al., 2015) as shown in Table 3. The different damage levels (*D0-D5*) refer both to the loss of functions and to the required recovery actions. We considered static scenarios, neglecting the times required to move from one state to another (e.g. cleaning times are much shorter than repair times).

Damage level:		**D0**	**D1**	**D2**	**D3**	**D4**	**D5**
Description:		**No damage**	**Cleaning required**		**Repair required**		**Beyond economic repair**
Power	**Function**	Fully functional	Temporary disruption		Disruption requiring repair		Permanent disruption
	Damage	No damage	No damage to components		Damage to critical components; long delays in receiving replacement components		Structural damage
	Thickness [mm]	0 (0-20)	5 (1-20)		20 (2-100)		> 500 (100-1000)
	Thickness [mm]	0 (0-5)	0.5 (0.1-10)	2 (1-20)	50 (10-100)	150 (50-300)	n/a

Table 3. Approximate values of dry ash thickness in relation to damage level and the functional states for power systems (modify from Jenkins et al., 2015).

3. Probabilistic damage scenarios

Probabilistic hazard scenarios for seismic ground shaking, tephra deposits and lava flows were calculated for different exposure times (T_E), with a view to comparing the different risk levels. Based on the historical seismic and eruptive activity of Etna, we considered exposure times in the order of decades for the hazards pertaining to strong earthquakes and lava flows from flank eruptions, and shorter exposures T_E (up to five years) for tephra deposition.

In detail, we considered exposure times of 10 and 30 years for probabilistic seismic scenarios and tephra load from flank activity, and 30 years for lava flow hazard from flank eruptions. The aggregated maps for tephra fall and lava flows were assessed considering exposure times respectively of 5 and 10 years, chosen as a balance between the different timescales of long-term flank eruptive activity and shorter-term summit activity (Cappello et al., 2025). As regards the exceeding probability (P_{EXC}), we considered values of 5% and 10%.

By combining the hazards, these different values of T_E and P_{EXC}, and the exposed elements, we therefore obtained 24 probabilistic risk scenarios (as detailed in Table 4), which were used to perform different conditional risk analyses.

Analyzing the values of the seismic, tephra fall and lava flow scenarios, we found that $T_E = 10$ years is a representative time for all three hazards. Below we present some examples of quantitative risk assessment, in particular analyses are presented by fixing the probability of excess and varying the values of danger intensity, and vice versa.

T_E	P_{EXC}	Hazard	Exposed element	
			Residential building	Power system
5 ye ars	5% and 10%	Tephra load (aggregated)	$X_{(5\%)}$, $X_{(10\%)}$	$X_{(5\%)}$, $X_{(10\%)}$
10 years	5% and 10%	Lava flow (aggregated)	$X_{(5\%)}$, $X_{(10\%)}$	$X_{(5\%)}$, $X_{(10\%)}$
		Tephra load (from flank vents)	$X_{(5\%)}$, $X_{(10\%)}$	$X_{(5\%)}$, $X_{(10\%)}$
		Seismic action	$X_{(5\%)}$, $X_{(10\%)}$	
30 years	5% and 10%	Lava flow (flank only)	$X_{(5\%)}$, $X_{(10\%)}$	$X_{(5\%)}$, $X_{(10\%)}$
		Tephra load (from flank vents)	$X_{(5\%)}$, $X_{(10\%)}$	$X_{(5\%)}$, $X_{(10\%)}$
		Seismic action	$X_{(5\%)}$, $X_{(10\%)}$	

Table 4. Probabilistic risk scenarios generated for residential buildings and power systems affected by volcanic hazards (tephra, lava and volcano-tectonic earthquakes), for different exposure times (T_E) and exceeding probabilities (P_{EXC}). Aggregated maps for tephra and lava hazard consider both the flank and summit activity.

3.1 Conditional risk analysis with fixed exceedance probability

Risk assessment was first carried out using fixed values of P_{EXC} and spatial variability of the hazard intensity, for each T_E. In the following, we present the results obtained considering residential buildings damaged by earthquakes and tephra loads for the municipality of Milo, and power distribution system covered by tephra flows for the whole area of the six municipalities.

Referring to the risk due to seismic hazard, it is possible to estimate the conditional risk value, expressed as the expected number of damaged buildings, using the methods illustrated in Section 2.1, both for masonry and reinforced concrete buildings, for each probability value of PGA provided by the probabilistic seismic hazard (see D'Amico et al., 2025). The expected number of damaged buildings with $P_{EXC} = 10\%$ and $T_E = 10$ and 30 years is illustrated in Table 5. Thanks to the method adopted for damage assessment that provide the distribution of buildings into the EMS-98 damage classes (*D1-D5*), it was possible to estimate the number of collapsed buildings (*D5*) and the heavy damaged buildings (*D5* + *D4*) in each census section. Other assessed risk indicators

are the number of unusable buildings, calculated as the weighted sum of buildings with heavy and substantial damage (60% *D3* + 100% *D4*), the number of victims (dead and injured), that can be associated with the heavy damage distribution (6% *D4* + 40% *D5*), and the number of homeless, calculated as 60% *D3* + 100% *D4* (all index are from Dolce et al., 2020).

Milo	T_E = 10 years	T_E = 30 years
Collapsed buildings	0.18	0.43
Heavy damaged buildings	1.17	1.85
Unusable buildings	2.23	2.65
Victims (dead and injured)	0.15	1.94
Homeless	2.54	6.31

Table 5. Expected annual average value of damaged buildings and number of involved residents due to seismic hazard evaluated for the municipality of Milo calculated with an exceeding probability P_{EXC} = 10% for two different exposition times: T_E = 10 and 30 years.

The probability of complete destruction of building roofs due to tephra fall was estimated using the method proposed in Section 2.2, considering the probabilistic distribution of loads in each census section, for different P_{EXC} and T_E.

The application of conditional risk analysis with fixed probability level enables a comparison of the risk associated with a multi-hazard scenario. For example, it is possible to calculate the highest level of damage (*D5*) for residential buildings under the actions of earthquakes and tephra loads during the same volcanic crisis. To facilitate comparison, the expected annual average values were calculated for a combination of T_E (5, 10 and 30 yrs) and P_{EXC} (5% and 10%) values. The results are presented in Table 6 for completely destroyed buildings of Milo. However, these values can vary significantly, making direct comparison challenging.

	P_{EXC} 5%			P_{EXC} 10%		
Buildings D5	**T_E = 5 years**	**T_E = 10 years**	**T_E = 30 years**	**T_E = 5 years**	**T_E = 10 years**	**T_E = 30 years**
tephra	0.8	0.02	0.02	0.01	0	0
earthquake	—	0.54	0.25	—	0.18	0.43

Table 6. Expected annual average value of the number of collapsed buildings (*D5*), due to seismic actions and tephra loads for different exposition time (T_E = 5, 10 and 30 years) and exceeding probability (P_{EXC} = 5% and 10%) for the municipality of Milo.

With reference to the highest levels of damage (*D5*), volcano related seismic activity represents the most significant source of risk, while the probability of tephra loads reaching a level to damage a roof is extremely low. It is noteworthy that lava flow scenarios presents exceedance probability values less than 5% in the considered area.

Social and economic losses are also sustained for lower levels of damage, which do not necessarily lead to the complete collapse of structures. In this case, other hazards, such as the presence of tephra thicknesses, increase their

potential for damage. In this regard, the potential damage to the power distribution system, including pylons and medium and high voltage substations, has been estimated for each value of the tephra loads, within the specified range, as illustrated in Table 3. Figure 3 shows the number of damaged components in a probabilistic tephra scenario at $T_E = 10$ years and $P_{EXC} = 10\%$, calculated for the entire area of the six municipalities. For instance, for tephra loads between 5 and 20 mm, there are 28 pylons and 297 transformers needing cleaning in order to overcome the potential for temporary inconveniences.

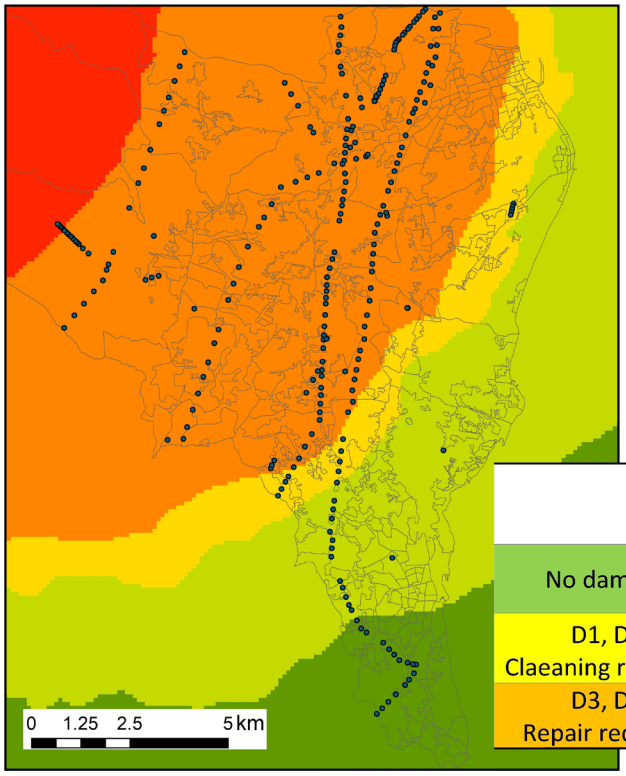

	Deposit [kg/m²]	Substation HV	Substation MV	Pylon
No damage	< 5	1		17
D1, D2 Claeaning required	5 - 20		297	28
D3, D4 Repair required	20 - 500	2	691	201

Figure 3. Distribution of expected tephra load with 10% of probability of exceedance over a 10-years exposure time (left) and assessment of the resulting damage to the power distribution system components (right). HV and MV refers to the high voltage and medium voltage substations, respectively. The background shapes (in gray) represents the census sections of the study area. Dots show the location of pylons.

3.2 Conditional risk analysis with fixed hazard intensity

Probabilistic risk scenarios can be alternatively produced analysing the variation of P_{EXC} for each fixed threshold value of intensity, e.g. for each T_E.

A probabilistic map of lava flow inundation is the simpler example of fixed intensity scenario, where the intensity measure is a binary variable indicating the presence of lava (without considering its thickness). In this case, the expected number of buildings damaged by the lava and the number of their inhabitants are calculated for those located in the invasion area.

As applicative example, considering a threshold of $P_{EXC} = 1\%$ and an exposure time of 10 years, only part of the urbanized area in Milo can be interested by a lava flow (see box in Fig. 4). In this case, the expected number of damaged buildings (~23) is calculated in proportion to the area of the section actually occupied by the lava.

Figure 4 illustrates the urbanized areas and the power distribution system (lines and pylons) that can be affected by lava flow as a function of varying exceedance probabilities at $T_E = 10$ years. As a result, only a couple of pylons are interested by the lava invasion with an exceeding probability less than 1% in the expected time of 10 years.

Conditional risk analysis with fixed hazard intensity are used to implement a target-based multi-hazard analysis (Garcia et al. 2025). Indeed, after that the single hazard results have been harmonized in a multi-hazard

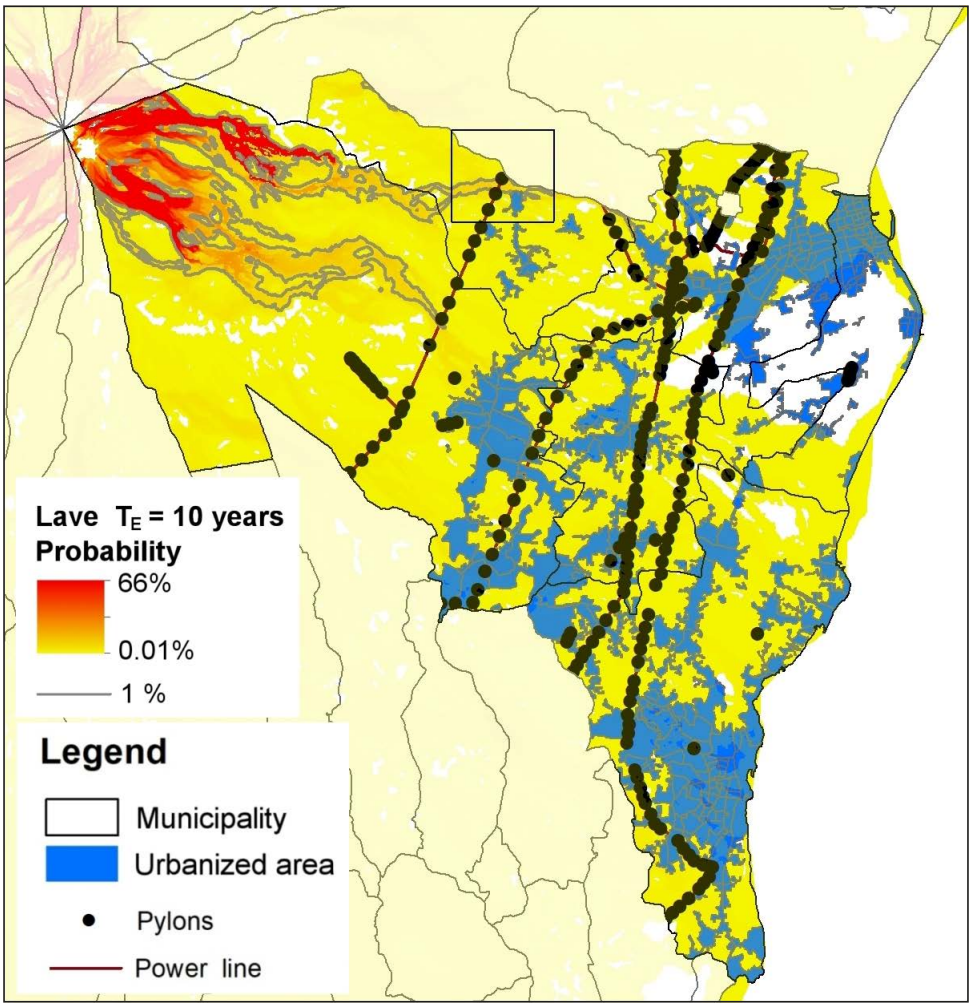

Figure 4. Lava flow hazard map at $T_E = 10$ years, showing the pylons and the buildings of Milo (inside the black box) inundated with an exceeding probability of 1%.

analysis, a target object of risk has to be introduced by the decision makers who identify a threshold value of accepted risk.

To illustrate the concept of conditional risk analysis with fixed hazard intensity, let's consider the case of assessing the level of damage of a power distribution system under threat of tephra loads. The probability of damage *D2*, which typically corresponds to a situation of onset of discomfort or unserviceability, can be estimated on the basis of a threshold value of the hazard parameters.

In the event of tephra fallout on a power distribution system, an ash loads equal or greater than 5 mm could have the potential to generate a temporary disruption, resulting in damage level *D1-D2* (Table 3). The generation of a fixed intensity scenario with tephra thickness higher than 5 mm (Fig. 5) enables the calculation of the various values of P_{EXC} at each point along the network where cleaning must be activated.

4. Discussion and conclusions

An organic multi-hazard risk assessment was only possible by implementing a complex methodology, such as the one proposed in the PANACEA project, where the volcanic hazards threatening the eastern area of Mt. Etna has been investigated organically and in detail for the first time.

Although it is possible to estimate risk values from hazard scenarios available in the literature or from previous studies, only the development of congruent scenarios, based on the most recent data, calculated with comparable resolutions on the same area and harmonized in a common format, can allow a consequent risk comparison. Furthermore, as risk estimates must also meet target-based requirements, they are therefore highly dependent on

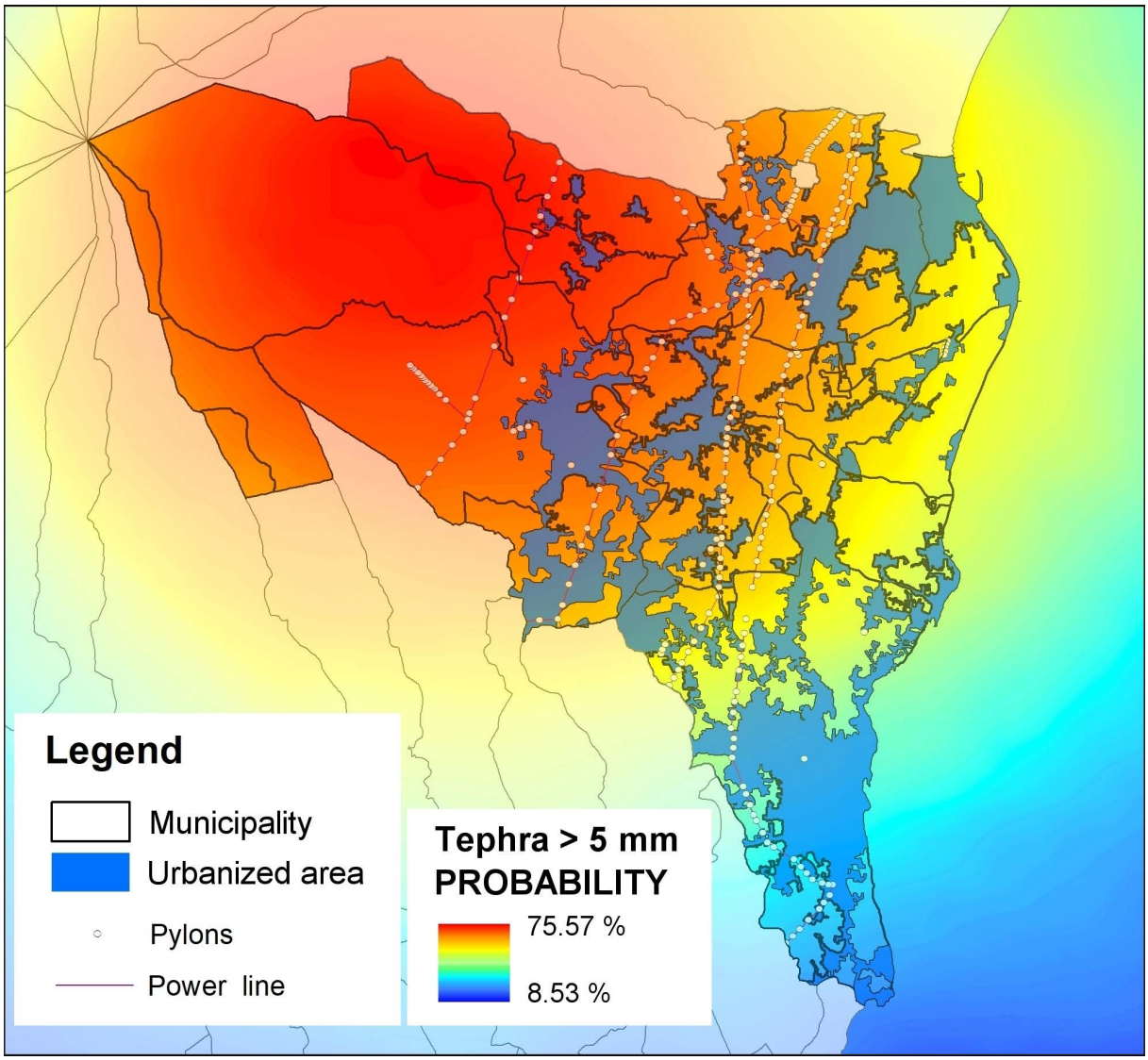

Figure 5. Fixed intensity scenarios for tephra loads equal to or greater than 5 mm, assumed as the threshold value for cleaning action of power systems.

the exposed elements. For all these reasons, the issue of multi-hazard risk assessment is a complex and integrated analysis that requires control and ensured consistency of all its steps, from the beginning to the end of the process.

In this contribution, a risk assessment was carried out for residential buildings and power distribution system taking into account the hazards due to lava flows, tephra deposits and volcano-tectonic earthquakes.

The probabilistic risk scenarios were evaluated both under the condition of fixed probability and fixed intensity values. In the first case, it was necessary to select values of exceeding probability and to determine the corresponding value of the hazard indicator (intensity measure) at each point within the studied area (i.e. the thickness of the tephra deposit, the peak ground acceleration, and the presence or absence of lava). Once the P_{EXC} value has been set for each T_E, it was possible to compare the expected damage values over the area and identify their relative weight. While tephra deposits can pose significant disruption and require extensive cleanup in the short term (as demonstrated by recent events in 2024), this analysis shows that a longer time horizon is required for tephra to become a significant contributor to heavy damage (Mereu et al., 2024). Currently, among the considered hazard, local earthquakes are the primary cause of heavy damage, causing the collapse of buildings (see Table 6).

Fixed probability risk scenarios allow for the planning of long-term interventions or the evaluation of the probability of interventions in the near future.

The availability of organic and structured multi-hazard data allows the estimation of probabilistic risk scenarios with fixed intensity values, i.e. the setting of hazard indicator values for each exposed element at the minimum

threshold above which damage occurs. The probability of occurrence can then be calculated, which varies throughout the whole territory. Once the level of damage that can be tolerated by each element has been established, it is possible to evaluate the probability of each hazard affecting that element and to prepare the necessary actions accordingly. This makes it possible to respond to the demands of decision-makers and administrators, especially on the choices to be made in the event of a crisis in the short term.

The presented results are few examples of the risk assessments carried out within the PANACEA project: however, these risk estimates are at an early stage due to the lack of organic data on the exposed elements and their vulnerability, and the lack of appropriately calibrated fragility models for the Etna area.

It is evident that the adopted working method facilitates in-depth studies in a modular manner, opening the way for numerous potential developments, including the incorporation of new hazards (e.g. flood, wildfire, etc.), the increase to new exposed elements and the interaction between hazard levels.

However, these risk analyses are an invaluable representation of the efforts invested in advanced simulations and high-level scientific research. These analyses are capable of providing useful data for land management in the context of natural hazard prevention, as well as for the management of remarkable seismic-volcanic emergencies.

Acknowledgements. This work was carried out within the PANACEA project that benefited from funding provided by the MIUR (Ministero Istruzione Università e della Ricerca) – Decreto MIUR 1118 del 04/12/2019, within the Pianeta Dinamico project. We acknowledge A. Torrisi of the Department of Civil Protection of Sicily (DPCR) for providing the 2002 AeDes data. We would like to express our gratitude to all the partners of the PANACEA project for their contributions to the development of this analysis. We also extend our sincere thanks to the referees for their valuable suggestions and constructive comments, which have greatly enhanced the quality of this work.

References

Alberico, I., P. Petrosino and L. Lirer (2011). Volcanic hazard and risk assessment in a multi-source volcanic area: the example of Napoli city (Southern Italy), Nat. Hazards Earth Syst. Sci., 11, 1057-1070, doi:10.5194/nhess-11-1057-2011.

Alcorn, R., K. S. Panter and P. V. Gorsevyki (2013). A GIS-based volcanic hazard and risk assessment of eruptions sourced within Valles caldera, New Mexico, J. Volcanol. Geothermal Res., 267, 1-14, doi:10.1016/j.jvolgeores.2013.09.005.

Alcozer-Vargas, N., M. P. Reyes-Hardy, A. Esquivel and F. Aguilera (2022). A GIS-based multi-hazard assessment at the San Pedro volcano, Central Andes, northern Chile, Front. Earth Sci., 10, 897315, doi:10.3389/feart.2022.897315.

Andronico, D., S. Scollo, S. Caruso and A. Cristaldi (2008). The 2002-03 Etna explosive activity: tephra dispersal and fea-tures of the deposits, J. Geophys. Res. Solid Earth, 113, B04209, doi:10.1029/2007JB005126.

Azzaro, R., S. D'Amico, R. Rotondi, T. Tuvè et al. (2013). Forecasting seismic scenarios on Etna volcano (Italy) through probabilistic intensity attenuation models: a Bayesian approach, J. Volcanol. Geotherm. Res., 251, 149-157, doi:10.1016/j.jvolgeores.2012.07.011.

Azzaro, R. and S. D'Amico (2014). Catalogo Macrosismico dei Terremoti Etnei (CMTE), 1633-2023, Data set, Istituto Nazionale di Geofisica e Vulcanologia (INGV), doi:10.13127/cmte, https://www.ct.ingv.it/macro/etna.

Baggio, C., A. Bernardini, R. Colozza, L. Corazza et al. (2007). Field Manual for post-earthquake damage and safety assessment and short term countermeasures (AeDES), in JRC Scientific and Technical Reports A.V. Pinto and F. Taucer (Eds.), Joint Research Centre, Institute for the Protection and Security of the Citizen, 100.

Bonadonna C., S. Biass, E. S. Calder, C. Frischknecht et al. (2018). 1st IAVCEI/GVM Workshop: From Volcanic Hazard to Risk Assessment, Geneva 27-29 June 2018, https://theghub.org/resources/4498/supportingdocs.

Bonadonna, C., C. B. Connor, B. F. Houghton, L. Connor et al. (2005). Probabilistic modeling of tephra dispersal: Hazard assessment of a multiphase rhyolitic eruption at Tarawera, New Zealand. J. Geophys. Res., 110, B03203, doi:10.1029/2003JB002896.

Bonadonna, C., C. Frischknecht, S. Menoni, F. Romerio et al. (2021). Integrating hazard, exposure, vulnerability and resilience for risk and emergency management in a volcanic context: the ADVISE model, J. Appl. Volcanol., 10, 7, doi:10.1186/s13617-021-00108-5.

Cappello, A., G. Bilotta and G. Ganci (2022). Modeling of geophysical flows through GPUFLOW, Appl. Sci., 12, 4395, doi:10.3390/app12094395.

Cappello, A., G. Bilotta, F. Zuccarello, C. Proietti et al. (2025). An improved methodology for lava flow hazard mapping at etna volcano, Ann. Geophys., 68, 1, doi:10.4401/ag-9157.

Centorrino, V., G. Bilotta, A. Cappello, G. Ganci et al. (2021). A particle swarm optimization-based heuristic to optimize the configuration of artificial barriers for the mitigation of lava flow risk, Environ. Model. Softw., 139, 105023, doi:10.1016/j.envsoft.2021.105023.

D'Amico, V. and D. Albarello (2008). SASHA: a computer program to assess seismic hazard from intensity data, Seismol. Res. Lett., 79, 5, 663-671, doi:10.1785/gssrl.79.5.663.

D'Amico, S., R. Azzaro, G. Tusa, T. Tuvè et al. (2025). Volcano-tectonic seismicity and related hazard: a component of the multi-hazard assessment in the highly exposed region of Mt. Etna (Italy), Ann. Geophys., 68, 1, doi:10.4401/ag-9152.

D'Amico, S., F. Meroni, M. L. Sousa and G. Zonno (2016). Building vulnerability and seismic risk analysis in the urban area of Mt. Etna volcano (Italy), Bull. Earthq. Eng., 14, 1797-1811, doi:10.1007/s10518-015-9804-4.

Del Negro, C., A. Cappello, G. Bilotta, G. Ganci et al. (2019). Living at the edge of an active volcano: Risk from lava flows on Mt. Etna, Bull. Geol. Soc. Am.,132, 7-8, 1615-1625, doi:10.1130/B35290.1.

Dolce, M., A. Prota, B. Borzi, F. da Porto et al. (2021). Seismic risk assessment of residential buildings in Italy, Bull. Earthq. Eng., 19, 2999-3032, doi:10.1007/s10518-020-01009-5.

Faccioli E., V. Pessina, G. M. Calvi and B. Borzi (1999). A study of damage scenarios for residential buildings in Catania city, J. Seismol., Special Issue, 3, 3, 327-343, doi:10.1023/A:1009856129016.

Ganci, G., G. Bilotta, M. Mangiameli, G. Mussumeci et al. (2023a). Roof covering classification using skysat multispectral imagery, in American Institute of Physics Conference Series, 2849, 1, doi:10.1063/5.0163757.

Ganci, G., A. Cappello and M. Neri (2023b). Data Fusion for Satellite-Derived Earth Surface: The 2021 Topographic Map of Etna Volcano, Remote Sens., 15, 198, doi:10.3390/rs15010198.

Garcia, A., L. Sandri, V. Pessina, F. Meroni et al. (2025) A target-based, multi-hazard assessment approach as a tool for supporting decision-making in volcanic areas: a case study in Mt. Etna, Italy, Ann. Geophys., 68, doi:10.4401/ag-9173.

Grünthal, G. (1998). European macroseismic scale 1998 (EMS-98), in Cahiers du Centre Européen de Géodynamique et de Séismologie, Luxembourg, Conseil de l'Europe, 15.

ISTAT (2011). 15° Censimento generale della popolazione e abitazioni, http://dati-censimentopopolazione.istat.it/Index.aspx?lang=it.

Jenkins, S. F., T. M. Wilson, C. Magill, V. Miller et al. (2015). Volcanic ash fall hazard and risk. Global volcanic hazards and risk, 173-222, Cambridge University Press, doi:10.1017/CBO9781316276273.005.

Lagomarsino, S., S. Cattari and D. Ottonelli (2021). The heuristic vulnerability model: fragility curves for masonry buildings, Bull. Earthq. Eng., 19, 3129-3163, doi:10.1007/s10518-021-01063-7.

Loughlin, S. C., R. S. J. Sparks, S. K. Brown, S. Jenkins et al. (2015). Global volcanic hazards and risk, Cambridge University Press, doi:10.1017/CBO9781316276273.

Martí Molist, J. (2017). Assessing Volcanic Hazard: A Review, in Oxford Handbook Topics in Physical Sciences, Online edition, Oxford Academic, 6 Sept. 2017, doi:10.1093/oxfordhb/9780190699420.013.32.

Martín-Raya, N., J. Díaz-Pacheco and A. López-Díez (2024). A Multi-hazard risk assessment analysis in La Palma: an approach for risk mitigation, Geoenviron. Disasters, 11, 33, doi:10.1186/s40677-024-00296-3.

Meredith, E. S., S. F. Jenkins, J. L. Hayes, N. I. Deligne et al. (2022). Damage assessment for the 2018 lower East Rift Zone lava flows of Kīlauea volcano, Hawaii, Bull. Volcanol., 84, 7, 65, doi:10.1007/s00445-022-01568-2.

Mereu, L., M. Stocchi, A. Garcia, M. Prestifilippo et al. (2024). Estimating the mass of tephra accumulated on roads to best manage the impact of volcanic eruptions: the example of Mt. Etna, Italy, EGUsphere, preprint, doi:10.5194/egusphere-2024-2028, 2024.

Meroni, F., G. Zonno, R. Azzaro, S. D'Amico et al. (2016). The role of the urban system dysfunction in the assessment of seismic risk in the Mt. Etna area (Italy), Bull. Earthq. Eng., 14, 1979-2008, doi:10.1007/s10518-015-9780-8.

Meroni, F., V. Pessina, R. Azzaro, S. D'Amico et al. (2022). From seismic damage assessment to a risk volcanic scenarios in the area of Mount Etna (Sicily), 2nd Int. Conf. on Urban Risk, 30 june-2 July, Lisbon, 345-348.

Neri, M., F. Casu, V. Acocella, G. Solaro et al. (2009). Deformation and eruptions at Mt. Etna (Italy): a lesson from 15 years of observations, Geophys. Res. Lett., 36, L02309, doi:10.1029/2008GL036151.

Neri, M., V. Acocella, B. Behncke, V. Maiolino et al. (2005). Contrasting triggering mechanisms of the 2001 and 2002-2003 eruptions of Mount Etna (Italy), J. Volcanol. Geotherm. Res., 144, 235-255, doi:10.1016/j.jvolgeores.2004.11.025.

Pareschi, M. T., I. Cavarra, M. Favalli, F. Giannini et al. (2000). GIS and volcanic risk management, Nat. Hazard., 21, 361-379, doi:10.1023/A:1008016304797.

Pessina, V. (1999). Empirical prediction of the ground shaking scenario for the Catania area, J. Seismol., Special Issue, 3, 3, 265-277, doi:10.1023/a:1009828304521.

Pessina, V., A. Garcia, F. Meroni, L. Sandri et al. (2022). From multi-hazard to multi-risk at Mount Etna: approaches and strategies of the PANACEA project, 3rd Int. Workshop on Natural Hazards, 26-27 May, Terceira Island, Azores, 37-40, doi:10.1007/978-3-031-25042-2_7.

Pessina, V., F. Meroni, R. Azzaro and S. D'Amico (2021). Applying simulated seismic damage scenarios in the volcanic region of Mount Etna (Sicily): a case-study from the MW 4.9, 2018 earthquake, Front. Earth Sci., 9, 629184, doi:10.3389/feart.2021.629184.

Pessina, V., F. Meroni, E. Varini, M. Longoni et al. (2024). Towards a multi-risk deterministic scenario in the Mt. Etna area, The 42nd National Conference of the GNGTS, 13-16 February, Ferrara, 100-105, doi:10.13120/dna7-2n16.

Rosti, A., C. Del Gaudio, M. P. Rota, P. Ricci et al. (2021). Empirical fragility curves for Italian residential RC buildings, Bull. Earthq. Eng., 19, 3165-3183, doi:10.1007/s10518-020-00971-4.

Rotondi, R., E. Varini and C. Brambilla (2016). Probabilistic modelling of macroseismic attenuation and forecast of damage scenarios, Bull. Earthq. Eng., 14, 7, 1777-1796, doi:10.1007/s10518-015-9781-7.

Sandri, L., A. Garcia, C. Proietti, S. Branca et al. (2024). Where will the next flank eruption at Etna occur? An updated spatial probabilistic assessment, Nat. Hazards Earth Syst. Sci., 24, 4431-4455, doi:10.5194/nhess-24-4431-2024.

Scollo, S., M. Prestifilippo, G. Spata, M. D'Agostino et al. (2009). Monitoring and forecasting Etna volcanic plumes, Nat. Hazards Earth Syst. Sci., 9, 1573-1585, doi:10.5194/nhess-9-1573-2009.

Scollo, S., M. Coltelli, C. Bonadonna and P. Del Carlo (2013). Tephra hazard assessment at Mt. Etna (Italy) in Natural Hazards and Earth System Sciences Discussions, 1, 3, 2945-2981, doi:10.5194/nhessd-1-2945-2013.

Scollo, S., C. Bonadonna, A. Garcia, L. Mereu et al. (2025) New developments in the estimation of tephra fallout hazard at Mt. Etna, in Italy, during the PANACEA project, Ann. Geophys., 68, 1, doi:10.4401/ag-9174.

Sigbjörnsson, R., G. Zonno and C. S. Oliveira (2016). Special Issue on The European project UPStrat-MAFA: Urban disaster prevention strategies using MAcroseismic Fields and FAult Sources, Bull. Earthq. Eng., 14, 7.

Spence, R. and B. L. Brun (2006). Preface, Bull. Earthq. Eng., 4, 319-321, doi:10.1007/s10518-006-9019-9.

Spence, R., I. Kelman, S. Petrazzuoli and G. Zuccaro (2005). Residential Buildings and Occupant Vulnerability to Tephra Fall, Nat. Hazards Earth Syst. Sci., 5, 477-494, doi:10.5194/nhess-5-477-2005.

Torrisi, A. (2018). AeDES forms for post-earthquake damage and safety assessment and short term countermeasures collected after the October 2002 Etna earthquakes, Regione Siciliana, Dipartimento della Protezione Civile, Servizio Rischio Sismico e Vulcanico S.03, Nicolosi, Italy, in Italian.

Weir, A. M., M. T. Wilson, M. S. Bebbington, S. Beaven et al. (2024). Approaching the challenge of multi-phase, multi-hazard volcanic impact assessment through the lens of systemic risk: application to Taranaki Mounga, Nat. Hazards, 120, 9327-9360, doi:10.1007/s11069-023-06386-z.

Zuccarello, F., M. de' Michieli Vitturi, T. Esposti Ongaro, G. Ganci et al. (2025). Dynamics and hazards of pyroclastic avalanches at Etna volcano (Italy), Ann. Geophys., 68, 1, doi:10.4401/ag-9158.

Zuccaro, G. and D. De Gregorio (2019). Impact assessments in volcanic areas – The Vesuvius and Campi Flegrei cases studies, Ann. Geophys., 62, 1, VO02, doi:10.4401/ag-7827.

***CORRESPONDING AUTHOR: Vera PESSINA**,
Istituto Nazionale di Geofisica e Vulcanologia,
Istituto Nazionale di Geofisica e Vulcanologia, Department of Milan, Milan, Italy
e-mail: vera.pessina@ingv.it